Published in final edited form as:
Sens Actuators B Chem. 2014 December 1; 204: 536–543. doi:10.1016/j.snb.2014.07.126.

Multichamber Multipotentiostat System for Cellular Microphysiometry

Eduardo A. Lima[1,2], **Rachel M. Snider**[3], **Ronald S. Reiserer**[2,4], **Jennifer R. McKenzie**[2,3], **Danielle W. Kimmel**[3], **Sven E. Eklund**[3], **John P. Wikswo**[2,4,5,6], and **David E. Cliffel**[2,3]

[1]Department of Earth, Atmospheric, and Planetary Sciences, Massachusetts Institute of Technology, Cambridge, Massachusetts. 02139, USA

[2]Vanderbilt Institute for Integrative Biosystems Research and Education, Vanderbilt University, Nashville, Tennessee. 37235, USA

[3]Department of Chemistry, Vanderbilt University, Nashville, Tennessee. 37235, USA

[4]Department of Physics and Astronomy, Vanderbilt University, Nashville, Tennessee. 37235, USA

[5]Department of Biomedical Engineering, Vanderbilt University, Nashville, Tennessee. 37235, USA

[6]Department of Molecular Physiology and Biophysics, Vanderbilt University, Nashville, Tennessee. 37235, USA

Abstract

Multianalyte microphysiometry is a powerful technique for studying cellular metabolic flux in real time. Monitoring several analytes concurrently in a number of individual chambers, however, requires specific instrumentation that is not available commercially in a single, compact, benchtop form at an affordable cost. We developed a multipotentiostat system capable of performing simultaneous amperometric and potentiometric measurements in up to eight individual chambers. The modular design and custom LabVIEW™ control software provide flexibility and allow for expansion and modification to suit different experimental conditions. Superior accuracy is achieved when operating the instrument in a standalone configuration; however, measurements performed in conjunction with a previously developed multianalyte microphysiometer have shown low levels of crosstalk as well. Calibrations and experiments with primary and immortalized cell cultures demonstrate the performance of the instrument and its capabilities.

Keywords

Keywords[1]: multipotentiostat; microphysiometry; microphysiology

Correspondence to: David E. Cliffel.

1. Introduction

Underutilized until recently [1, 2], microphysiometry substantially aids the study of cellular metabolism, which is a vast endeavor to explore how metabolic feedback influences cellular regulation [3]. Multianalyte microphysiometry, which uses multiple electrochemical sensors to simultaneously monitor the metabolism of cells, is uniquely poised to explore dynamic metabolic flux [4]. Concurrent recording in individual chambers is particularly advantageous, as it allows for biological replicates.

Microphysiometry was commercialized as the Cytosensor® (Molecular Devices), which uses light addressable potentiometric sensors (LAPS) to measure extracellular acidification rates (ECAR), providing correlations to changes in cellular metabolism [5]. Our multianalyte microphysiometer (MAMP) expanded upon the Cytosensor® with the addition of Pt electrodes into the sensor head for amperometric monitoring [4]. A potentiostat capable of measuring multiple working electrodes (WEs) within each electrochemical cell was required to further develop the MAMP as a viable tool for studying cellular metabolism.

Previous potentiostat designs have focused on portability [6-8], miniaturization [9-11], and energy efficiency [12-14]. While these are important features, they are not critical for metabolic studies conducted in research laboratories. Initial MAMPs utilized a CH Instruments 1030 multipotentiostat, which was limited to a common reference electrode (RE) and common counter electrode (CE), limiting measurement at one chamber [15]. Since then, the commercial availability of potentiostats with multiple RE and CEs, including the CHI 1030, has improved, but remain limiting in configurations allowing for multichamber microphysiometry. To measure multiple analytes in several electrochemical cells simultaneously, we created a multichamber multipotentiostat that also allows multichamber amperometric and potentiometric sensing. This instrument was built upon a custom modular framework that enables concurrent operation of up to eight modules controlled by a single computer. Two types of modules were designed: a multipotentiostat for amperometric measurements and a multichannel open circuit potential (OCP) module for potentiometric measurements.

We tested two configurations, each with a different technique to measure pH. The first configuration used the multipotentiostat module, with pH measurements performed by the Cytosensor® LAPS. These modules are capable of reliable measurements at a low frequency to minimize crosstalk when coupled with the high-frequency LAPS (10kHz) [5]. When used in combination with our multichamber multipotentiostat system, the Cytosensor®-dependent MAMP can simultaneously measure four-analyte metabolic responses in up to eight chambers.

In order to improve versatility, sensitivity, and eliminate interferences, we developed a second configuration with additional OCP modules to detect pH changes at an iridium oxide (IrOx) electrode incorporated into the MAMP sensor head. This also allowed for expansion of the MAMP technique to other platforms [16]. In this configuration, two multipotentiostat modules are replaced with two OCP modules, each containing three independent channels. Thus, one potentiometric pH sensor can be added to the three amperometric measurements,

allowing four-analyte detection in up to six electrochemical cells. In both configurations, the RE for each potentiostat module is shared with the potentiometric measurement of the LAPS or OCP module.

This instrument has been an invaluable tool for multianalyte microphysiometry, and has been used to study the detection of insulin secretion [17], pathways affected by cholera toxin exposure [18], glucose deprivation on neuronal metabolism [19, 20], and measurement of immunological responses [21, 22].

2. Instruments

2.1 Hardware

The multichamber multipotentiostat designed for use with the MAMP is an expansion of conventional bipotentiostat designs [23] incorporating stability control and a third WE held at the same potential as one of the independent WEs. Our multipotentiostat system consists of six parts, as depicted in Figure 1: passive backplane, power supply, configuration card, multipotentiostat modules, OCP modules, and control computer and DAQ card. It is housed in a 3U 19-inch subrack, which accepts ten 1.65″-wide card cages. Up to eight of these cages encase the multipotentiostat and OCP modules, and a wider (3.05″-wide) cage contains the power supply. The subrack was mounted in a 19-inch 3U tabletop rack enclosure (Figure S1).

The passive backplane (Figure S2) consists of a six-layer printed circuit board (PCB) with high-density connectors on both sides. On the front-side, eight male connectors accommodate mating for each module, whereas two male connectors on the back-side accommodate configuration card mating.

We used an open-frame dual-output regulated linear power supply capable of delivering +12V and -12V at 1.7A to ensure linear operation of the instrument within the DAQ cards ±10V range. A combination rocker/thermal circuit breaker switch located at the card cage front panel controls the power supply (Figure S3).

The configuration card (Figures 2 and S4) is responsible for distributing power to the backplane, routing backplane signal lines to the DAQ card and vice versa, optically isolating digital signals to and from the DAQ card, decoupling the potentiostat analog ground from the DAQ card analog ground, implementing a power-on sequencing scheme, implementing a six-bit data bus with two additional control bits, and providing control signals to reed relays that connect/disconnect electrodes to/from each module.

The data bus handles selection of sensitivity ranges as well as the saturation status and slot number. To maintain compatibility with E-series DAQ cards from National Instruments, we used 8-bit digital I/O, leading to the 6-bit bus concept. The use of a configuration card considerably simplifies adapting and expanding design, as it does not require backplane or module changes. The two control bits regulate whether the DAQ card is writing or reading information from the bus, in addition to regulating the state of reed relays on the modules. Although sensitivity settings are shared across modules, each of the WEs has separate sensitivity controls. There are four sensitivity ranges per electrode (1000, 100, 10, and

1nA/V), which are selectable via a pair of bits. By means of individually addressable lines, each module outputs a saturation status signal, which is fed to an input of an 8-line to 3-line priority encoder.

Digital signal isolation and level translation are accomplished by optoisolators and transistors. Digital signals coming from the 5V-logic DAQ card are converted to 12V CMOS logic, while signals coming from modules are converted to 5V-logic. For analog inputs, the DAQ card configuration operates in non-referenced single-ended mode, meaning the power supply ground is connected to an instrumentation amplifier input, while the module outputs are connected to other inputs through an analog multiplexer, both within the DAQ card. Finally, the goal of the power-on sequencing scheme is to ensure proper operation of CMOS analog switches.

Although tailored for specific applications, modifications are straightforward for implementation to true tri-potentiostat or other configurations, given that the circuit core is the same. For maximum performance, superior reliability, and compactness, nearly all components in the modules are surface mount technology (Figure S5).

Figure 3 depicts a potentiostat module connected to a MAMP chamber. An op-amp capable of handling capacitive loads drives the CE, while a high-impedance precision op-amp in buffer configuration senses the voltage at the RE, closing the feedback loop via adder circuit. Because the electrochemical cell is part of the feedback loop of the drive op-amp, oscillations may occur in some experimental setups despite the op-amp's internal compensation for capacitive loads [24, 25]. The nonlinear nature of electrochemical cells requires additional flexible compensation to stabilize the potentiostat circuit over a wide range of experimental conditions and to minimize the necessity of external components to tame oscillatory behavior.

We implemented an input-lag compensation scheme [26, 27] with four selectable resistors and a fixed capacitor. The tradeoff for enhanced stabilization is an increase in high-frequency noise, which is subsequently filtered out at the current-to-voltage (I-V) converters and voltage gain sections. The values for the capacitor and resistors were obtained empirically, as they were tailored to MAMP chambers.

Analog signals pertaining to the electrochemical cell and earth ground are routed to the 6-pin LEMO connector on the front panel through single-pole, single-throw shielded reed relays controlled by the configuration card. The relays electrically isolate the electrodes from the circuit when no measurement is occurring, while still closing the drive op-amp's feedback path to avoid saturation and damage. Each of these op-amps has an associated CMOS analog switch that selects the gain resistor according to digital signals from the configuration card data bus. The I-V converters implement first-order low-pass filters, with cutoff frequencies at 7.5Hz. I-V converter outputs are further amplified and filtered by separate gain stages.

As in a conventional bipotentiostat, Vc_1 controls the potential of WE1 with respect to RE via the CE. In our expanded bipotentiostat, WE2 is kept at the same potential as WE1. As shown in Figure 3, currents flowing in WE1 and WE2 are sensed using I-V converters kept

at virtual ground. A second control voltage Vc_2 is fed to a precision difference amplifier that sets the baseline voltage of the third I-V converter to Vc_2 - Vc_1. In this manner, the potential of WE3 with respect to RE is Vc_2, making it effectively independent of WE1, WE2, and Vc_1. Another precision difference amplifier is used to shift the output of the third I-V converter such that it is properly referenced to ground.

I-V converter inputs, as well as the buffer, are guarded to minimize signal degradation. An iR compensation scheme was not implemented because current levels in MAMP experiments are typically below 500nA and solution resistance in biological media is low. CE voltage is constantly monitored by a window detector circuit, which incorporates a timer mechanism to hold output status fixed for certain periods of time. This signal is monitored by the priority encoder in the configuration card, which detects saturation state and identifies where it has occurred.

Figure 4 depicts an OCP module. The OCP core detection circuitry is an extremely low input bias current instrumentation amplifier that allows implementation of guarding two input pins. The negative input connects to the RE through a shielded reed relay, whereas the positive input connects to the WE through a reed relay. The output of the instrumentation amplifier is low-pass filtered at 5Hz by a two-stage 4^{th}-order Butterworth analog filter, which presents a suitable balance between selectivity, passband flatness, and phase distortion. The multichannel OCP circuits were assembled on a two-layer custom PCB (Figure S6). In both designs, connections between the front panel LEMO connectors and the electrodes were made by a multiconductor shielded cable.

2.2 Computer control

The Cytosoft™ program controls pumps and temperature of the MAMP [5]. A separate computer was used to control the multichannel multipotentiostat *via* National Instruments DAQ cards and custom-designed LabVIEW™ software. For four-chamber MAMPs and multipotentiostats, either the PCI-6036E or PCI-6221 DAQ card was used, and in eight-channel systems the PCI-6229 was used. Standard National Instruments 68-pin shielded cables connected DAQ cards to the configuration card.

2.3 Software

Software was written for multichamber amperometric and potentiometric sensing (Figure S8 and S9), as well as for multipotentiostat calibration (Figure S10). The LabVIEW™ graphic interface can be easily edited for module reconfiguration. The program is defined by the National Instruments DAQ card, with signals sent to the analog in and out channels of the card. As detailed in Figure S7, the user selects current sensitivity, applied potentials to WEs, quiet time, sample interval, and run time. Upon initialization, communication is set up between the DAQ board and potentiostat. During data collection, the program reads values from the DAQ board, then converts and plots using calibration factors within the program. Once complete, the program saves the data in a retrievable format and resets the circuit board and instrument. Further details on both the sensing and calibration software can be found in the supplemental information.

2.4 Calibration of multipotentiostat modules

To calibrate each multipotentiostat module we used a “dummy cell” composed of four 0.1% 10MΩ resistors (Figure S11). Gain calibration provides accurate voltage-to-current conversion factors, to adjust voltage data readings from the DAQ card. Offset compensation further improves accuracy, since each op-amp in the signal chain and the DAQ card will inevitably add small offset voltages to control signals and output voltages.

To decouple gain calibration from offset compensation, the software commands the DAQ card to output an ac control signal. To obtain the calibration factor, the peak-to-peak amplitude of test voltage is divided by the nominal resistance between the RE and WE, providing current flowing through the latter. This number is divided by the peak-to-peak amplitude of the voltage signal read by the DAQ card, yielding the calibration factor in nA/V. When calibrating WE1 and WE2, the ac test signal is applied to Vc_1, whereas Vc_2 is set to 0V. When calibrating WE3, the scheme is reversed and the ac test signal is applied to Vc_2, while Vc_1 is kept at 0V.

The offset voltage of the DAQ card and drive op-amp when a potential is applied to the CE must be determined to optimize instrument performance. We decided to handle the offset voltage issue digitally, by compensating control voltage output by the DAQ card and subtracting any residual offset from the digitized data. We set both Vc_1 and Vc_2 to 0V and measured all offset voltages for each WE per module. WE1 and WE2 are averaged together, as they are both controlled by Vc_1. This small offset voltage will be subtracted from the intended value for Vc_1 during experiments. The control voltage Vc_2 is compensated in a similar manner. This offset compensation scheme is sufficient for most experiments, given typical noise levels. For critical experiments, the residual offset voltage for each electrode may be subtracted to attain a high degree of accuracy.

2.5 Calibration of OCP modules

Calibration and offset compensation of OCP modules are calculated using a battery-operated ancillary circuit containing high-accuracy, sub-band-gap voltage reference chips and precision resistor bridges. Voltages are fed sequentially to each of three channels of an OCP module through miniature test clips during measurements. Based on nominal and actual voltages, a best-fit line is calculated, providing offset voltage (intercept) and calibration factor (slope). Figure S12 shows sample calibration curves used to improve accuracy of the OCP modules. This calibration procedure is repeated for each OCP module.

2.6 Interference studies

Simultaneous operation of a high-frequency LAPS, which samples at 10 kHz, and the low-frequency multipotentiostat within a shared electrochemical cell introduces noise into measured signals for both instruments, thus noise contamination studies were performed. Sensor heads with bare Pt electrodes were assembled in MAMP chambers without cells, and test clips attached to measure current at the WEs. Our media, a modified RPMI 1640 media (1mM phosphate buffer, no sodium bicarbonate, and 5mM glucose) was perfused through the chamber at 100μL/min as the Cytosensor® and LabVIEW™ programs operated for repeated 5min intervals at a sampling frequency of 1Hz. WEs were held at potentials used

for MAMP experiments, +0.6V for WE1 and WE2, and -0.45V for WE3, with sensitivities set at 100nA/V. Signals from the last 100s from each interval at both instruments were used to calculate noise occurring from simultaneous use. Average current magnitude depends on electrode size and applied potential; for comparison, percent standard error was calculated.

The second configuration of the MAMP achieves potentiometric sensing with the potentiostat OCP module. For this configuration, a screen-printed multianalyte sensor (SPE) was designed in-house and printed by Pine Research Instrumentation [16]. One electrode on the SPE was plated with a pH-sensitive IrOx film [28]. The SPEs were placed in 10 mL media and both module types were connected to a shared Ag/AgCl (2M KCl) RE. LabVIEW™ recorded data during four 5min cycles, under three conditions: collecting both amperometric and OCP signals, collecting amperometric signals, and collecting OCP signals. Data from the last 100s of each interval were averaged. Average current magnitude depends on electrode size and applied potential, therefore the percent standard error was calculated for comparison.

2.7 MAMP amperometric testing of the multipotentiostat

Several configurations were used to measure the WEs' amperometric responses of modified sensor heads in the MAMP: sensors with and without enzyme films and with enzyme films in the presence of cells. In all tests, WE1 and WE2 were held at +0.6V and WE3 was held at -0.45V *vs.* the MAMP Ag/AgCl (2M KCl) reference. Peristaltic flow was initiated first (100μL/min), followed by the multipotentiostat program 40s later.

Sensors modified to detect glucose, lactate, and oxygen were placed in the MAMP. Current response was recorded as media perfused in the chamber and the glucose and lactate electrodes were calibrated through perfusion of media spiked with increasing amounts of glucose and lactic acid.

The sensors and potentiostat were used to measure flux of glucose, lactate, and oxygen from live cells. Pheochromocytoma cells, PC-12 (CRL-1721, American Type Culture Collection), were prepared for use in the MAMP as previously described [18]. Concurrent measurements occurred while the chamber was perfused with media for 80min. Zero metabolic activity was achieved by perfusing 108μM alamethicin in media for 40min, and subsequent calibrations occurred, as in the no-cell experiment.

2.8 Simultaneous testing of amperometric and OCP modules of the multipotentiostat with the MAMP

In order to test performance of the OCP module in MAMP experiments, WE1 in the MAMP sensor head was plated with an IrOx film instead of glucose oxidase. The OCP module was tested using cortical cultures from day 18 Sprague-Dawley rats prepared as previously described [19]. Oxygen consumption and lactate production were measured with amperometric modules, and acid production was measured with the Cytosensor® and OCP modules.

The Cytosensor® and potentiostat were started as the chamber was perfused with media for 2.5hrs. At zero metabolic activity, sensors were calibrated via media perfusion with added lactate and known pH.

We modified the surfaces of a six-sensor array of multianalyte SPEs for detection of glucose, lactate, oxygen, and pH. Each sensor was modified with a Ag/AgCl layer to act as a quasi-reference. The potentiostat was used to simultaneously measure these analytes at all six sensors in 1mM phosphate buffer with 120mM KCl (PBS) while glucose, sodium lactate, and HCl were added in a step-wise fashion to calibrate the sensors. For simplicity, all six sensors were submerged in a bulk solution of PBS.

3. Results and Discussion

3.1 Interference

Interference studies determined noise contamination from simultaneous multipotentiostat and Cytosensor® operation. The standard error in the signal of LAPS alone was 0.10mV and 0.28±0.03mV during simultaneous amperometric measurements with the potentiostat. Given that the total change in potential during stop-flow due to acidification can be on the order of 1mV, this increase might adversely affect accuracy of ECAR measurements in less metabolically active cell lines. No significant noise difference in the multipotentiostat signals was observed, given the 3.5±1.4% standard error when the LAPS was simultaneously measuring and 3.3±1.7% error when the multipotentiostat was working independently.

Interference studies were also conducted with multipotentiostat and OCP modules to determine noise contamination from simultaneous operation. No significant increases in noise were observed in either signal when sampled together. Signals of the multipotentiostat and OCP modules had a standard error of 1.2±0.8% and 0.11±0.06%, respectively. Independently, signals of the multipotentiostat and OCP modules had a standard error of 1.0±0.6% and 0.027±0.004%, respectively. Peristaltic pumps were not used for this test, likely resulting in lower noise and standard error. These studies demonstrated that the multipotentiostat module is not significantly affected by simultaneous operation of a high-frequency Cytosensor® or by addition of the OCP module.

3.2 Amperometric testing of the multipotentiostat with the MAMP

Amperometric response of a modified sensor head with bare Pt electrodes without cells is shown in Figure 5. WE1 and WE2 current response is similar, which is expected of similar sized electrodes. During stop flow, decrease in current magnitude at WE1 and WE2 is due to the depletion of electroactive species in the media oxidized at the bare electrodes. The decrease in current magnitude of WE3 is due to the depletion of oxygen through electrochemical reduction. Peristaltic pump noise is evident during flow.

Figure S13 depicts currents measured at a modified sensor head with enzyme films, without cells. The current observed while media is perfused through the chamber is constant. As previously detailed, increasing concentrations of glucose and lactate are perfused through the chamber, resulting in increased current magnitude at the respective electrodes.

Additionally, signals at the bare Pt oxygen electrode (WE3) remain constant throughout the experiment as dissolved oxygen in the media is reduced at the electrode.

Figure 6 displays amperometric response of a modified sensor head with enzyme films with cells in one of four simultaneously measured channels. During metabolic activity, the magnitude of oxidation current at the lactate electrode increased during the stop-flow (production), and the magnitudes of currents at the glucose electrode and bare Pt oxygen electrode decreased (consumption). After alamethicin treatment, cells have zero metabolic activity. As such, any changes in current are due to the sensors' background currents.

3.3 Combined amperometric and OCP experiments

The OCP module was tested while measuring metabolic rates of primary neurons and glia co-cultures. Cells and sensors were prepared as described (Section 2.8). Figure 7 shows the simultaneous measurement of lactate, oxygen, and pH using the MAMP and the amperometric and OCP modules of the potentiostat in one of four simultaneously measured channels. The OCP module allowed for detection of acid independently of the Cytosensor®, and in conjunction with the IrOx electrode, yielded low-noise ECAR.

The surfaces of a six-sensor array of multianalyte SPEs were modified for detection of glucose, lactate, oxygen, and pH and calibrated simultaneously (Figure 8). All six amperometric and two OCP modules were able to monitor simultaneously, yielding 24 total signals. Each 4-analyte sensor was biased against its own Ag/AgCl quasi-reference. Variations in signals are due to differences in the sensor modifications. Any module variations are negligible compared to measurements being performed for microphysiometry.

Conclusions

We have developed a versatile, affordable, multichamber multipotentiostat system capable of simultaneously measuring amperometric responses of three WEs in combination with potentiometric responses. The multipotentiostat works with software selectable sensitivities of 1, 10, 100, or 1000nA/V. pH measurements are done at a fixed sensitivity range of ±1.0V.

This multipotentiostat instrument is applicable to experimental systems requiring simultaneous amperometric and potentiometric measurements in multiple electrochemical cells. The current design is limited to the application of two potentials; however, more analytes are possible by functionalizing sensors to use similar reduction or oxidation potentials. Design modification of the multipotentiostat cards to implement a tri-potentiostat would be straightforward.

This multipotentiostat increases the number of simultaneously used MAMP chambers from one to eight, allowing for concurrent testing of multiple cell types, exposures, or simultaneous parallel replicate experiments. This instrumentation has been vital to the development of multianalyte microphysiometry, enabling a wide range of metabolic research studies. Additionally, development of a six-chamber, SPE-based MAMP, which utilizes six multipotentiostat modules and two 3-channel OCP modules, is currently in its final stages.

Supplementary Material

Refer to Web version on PubMed Central for supplementary material.

Acknowledgments

This work is a component of the Massively-Parallel, Multiphasic Cell Biological Activity Detector (MP^{2}CBAD) Project, supported in part by DARPA/ONR contract N66001-01-C-8064, the Vanderbilt Institute for Integrative Biosystems Research and Education (VIIBRE), and grants from the National Institutes of Health/National Institute of Allergy and Infectious Diseases (U01AI061223) and the Defense Threat Reduction Agency (HDTRA1-09-1-0013). R.M. Snider gratefully acknowledges the support from the Chemical Biology Interface Training Grant at Vanderbilt supported by NIH T32 GM065086. We thank Shellie Richards, Allison Price, and Don Berry for editorial assistance.

References

1. Ray LB. Metabolism Is Not Boring. Science. 2010; 330:1337. [PubMed: 21127242]
2. Wong W. Focus Issue: Metabolic Signals. Science Signaling. 2010; 3:eg12. [PubMed: 21139135]
3. McKnight SL. On Getting There from Here. Science. 2010; 330:1338–9. [PubMed: 21127243]
4. McKenzie, JR.; Cliffel, DE.; Wikswo, JP. Electrochemical Monitoring of Cellular Metabolism. In: Savinell, R.; Ota, K.; Kreysa, G., editors. Encyclopedia of Applied Electrochemistry. Springer-Verlag; 2013. SpringerReference
5. Hafner F. Cytosensor((R)) Microphysiometer: technology and recent applications. Biosensors and Bioelectronics. 2000; 15:149–58. [PubMed: 11286332]
6. Kwakye S, Baeumner A. An embedded system for portable electrochemical detection. Sensors and Actuators B. 2007; 123:336–43.
7. Christidis K, Gow K, Robertson P, Pollard P. Intelligent potentiostat for identification of heavy metals in situ. Review of Scientific Instruments. 2006; 77:014103.
8. Avdikos EM, Prodromidis MI, Efstathiou CE. Construction and analytical applications of a palm-sized microcontroller-based amperometric analyzer. Sensors and Actuators B. 2005; 107:372–8.
9. Kimura M, Bundo K, Imuro Y, Sagawa Y, Setsu K. Chronoamperometry Using Integrated Potentiostat Consisting of Poly-Si Thin-Film Transistors. IEEE Electron Device Letters. 2011; 32:212–4.
10. De Venuto, D.; Torre, MD.; Boero, C.; Carrara, S.; De Micheli, G. Sensors 2010. IEEE; Piscataway, N.J.: 2010. A novel multi-working electrode potentiostat for electrochemical detection of metabolites; p. 1572-7.
11. Vergani M, Carminati M, Ferrari G, Landini E, Caviglia C, Heiskanen A, et al. Multichannel Bipotentiostat Integrated With a Microfluidic Platform for Electrochemical Real-Time Monitoring of Cell Cultures. IEEE Transactions on Biomedical Circuits and Systems. 2012; 6:498–507. [PubMed: 23853236]
12. Martin SM, Gebara FH, Strong TD, Brown RB. A Fully Differential Potentiostat. IEEE Sensors Journal. 2009; 9:135–42.
13. Stanacevic M, Murari K, Rege A, Cauwenberghs G, Thakor NV. VLSI Potentiostat Array With Oversampling Gain Modulation for Wide-Range Neurotransmitter Sensing. IEEE Transactions on Biomedical Circuits and Systems. 2007; 1:63–72. [PubMed: 23851522]
14. Steinberg MD, Lowe CR. A micropower amperometric potentiostat. Sensors and Actuators B. 2004; 97:284–9.
15. Eklund SE, Cliffel DE, Kozlov E, Prokop A, Wikswo J, Baudenbacher F. Modification of the Cytosensor™ microphysiometer to simultaneously measure extracellular acidification and oxygen consumption rates. Analytica Chimica Acta. 2003; 496:93–101.
16. Hiatt LA, McKenzie JR, Deravi LF, Harry RS, Wright DW, Cliffel DE. A printed superoxide dismutase coated electrode for the study of macrophage oxidative burst. Biosensors and Bioelectronics. 2012; 33:128–33. [PubMed: 22257735]

17. Snider RM, Ciobanu M, Rue AE, Cliffel DE. A multiwalled carbon nanotube/dihydropyran composite film electrode for insulin detection in a microphysiometer chamber. Analytica Chimica Acta. 2008; 609:44–52. [PubMed: 18243872]
18. Snider RM, McKenzie JR, Kraft L, Kozlov E, Wikswo JP, Cliffel DE. The effects of Cholera Toxin on cellular energy metabolism. Toxins. 2010; 2:632–48. [PubMed: 22069603]
19. Zeiger SLH, McKenzie JR, Stankowski JN, Martin JA, Cliffel DE, McLaughlin B. Neuron specific metabolic adaptations following multi-day exposures to oxygen glucose deprivation. Biochimica et Biophysica Acta - Molecular Basis of Disease. 2010; 1802:1095–104.
20. McKenzie JR, Palubinsky AM, Brown JE, McLaughlin B, Cliffel DE. Metabolic Multianalyte Microphysiometry Reveals Extracellular Acidosis is an Essential Mediator of Neuronal Preconditioning. ACS Chemical Neuroscience. 2012; 3:510–8. [PubMed: 22860220]
21. Kimmel DW, Meschievitz ME, Hiatt LA, Cliffel DE. Multianalyte Microphysiometry of Macrophage Responses to Phorbol Myristate Acetate, Lipopolysaccharide, and Lipoarabinomannan. Electroanalysis. 2013; 25:1706–12.
22. Shinawi TF, Kimmel DW, Cliffel DE. Multianalyte Microphysiometry Reveals Changes in Cellular Bioenergetics Upon Exposure to Fluorescent Dyes. Analytical Chemistry. 2013; 85:11677–80. [PubMed: 24228839]
23. Bard, AJ.; Faulkner, LR. Electrochemical Methods: Fundamentals and Applications. New York: John Wiley and Sons, Inc; 2001.
24. Harrar JE, Pomernac CL. Linear and Nonlinear-System Characteristics of Controlled-Potential Electrolysis Cells. Analytical Chemistry. 1973; 45:57–79.
25. Greef R. Instruments for Use in Electrode Process Research. Journal of Physics E: Scientific Instrumentation. 1978; 11:1–12.
26. Franco, S. Design with operational amplifiers and analog integrated circuits. New York: McGraw-Hill; 2002.
27. Mancini, R. Op amps for everyone: design reference. Boston: Newnes; 2003.
28. Marzouk SAM, Ufer S, Buck RP, Johnson TA, Dunlap LA, Cascio WE. Electrodeposited Iridium Oxide pH Electrode for Measurement of Extracellular Myocardial Acidosis during Acute Ischemia. Analytical Chemistry. 1998; 70:5054–61. [PubMed: 9852787]

Abbreviations

MAMP	Multianalyte Microphysiometer
LAPS	Light addressable potentiometric sensors
ECAR	Extracellular acidification rate
WE	Working electrode

Biographies

Eduardo A. Lima received his PhD in electrical engineering in Brazil at the Catholic University of Rio de Janeiro in 2001. From there he worked as a postdoctoral fellow at the Instituto de Matemática Pura e Aplicada before coming to Vanderbilt University as a research associate in the Department of Physics and Astronomy. In 2006 he joined the Massachusetts Institute of Technology as a research scientist in the Department of Earth, Atmospheric and Planetary Sciences. His current research focuses on the development of inverse problem techniques and instrumentation for conducting paleomagnetic studies of rocks on submillimeter scales.

Rachel M. Snider is currently a postdoctoral researcher at the BioTechnology Institute of University of Minnesota in the lab of Dr. Daniel Bond, studying the mechanism of extracellular microbial electron transfer. Dr. Snider did her doctoral research in the laboratory of Dr. David Cliffel at Vanderbilt University, developing electrochemical methods for measuring cellular response to toxins. After her doctoral work, she worked as a National Research Council research associate at the Naval Research Laboratory. There she worked on deploying benthic microbial fuel cells for long term sustained power generation. Dr. Snider is an avid Auburn football and Nashville Predators hockey fan.

Ronald S. Reiserer is the Laboratory Manager for the Vanderbilt Institute for Integrative Biosystems Research and Education (VIIBRE). He has an extensive background in the application of technology to solving practical problems, from industrial signaling and control, mechanical and fluid power transfer, well drilling, crop irrigation, livestock watering systems, large-scale replica fabrication, and automated information systems to conceptual design, prototyping, and production of electronics and mechanical sensing devices. His current work focuses on soft- and hard-lithographic fabrication of BioMEMS devices, microprocessors for controlling microfluidic pumps and valves, and other micro-scale experimental apparatus with matched sensing and control systems, and their application to problems in cell biology and organs-on-chips.

Jennifer R. McKenzie received her PhD in chemistry under the advisement of Dr. David Cliffel at Vanderbilt University in 2011. Her doctoral research focused on using electrochemical sensors to perform real-time toxicology by monitoring cellular metabolism. She spent a year as a Postdoctoral Associate for Dr. Chenzong Li in the Biomedical Engineering Department at Florida International University. During this time she developed novel electrochemical sensors for investigations of neuronal disease. In 2012, Dr. McKenzie returned to Vanderbilt as a Postdoctoral Scholar to design and implement the analytical instrumentation required to monitor the cellular changes occurring in Organ on Chip bioreactors.

Danielle W. Kimmel received her PhD in chemistry under the advisement of Dr. David Cliffel at Vanderbilt University in 2012. Her doctoral work focused on understanding the metabolic responses to immune and cancer cells undergoing oxidative burst via various oxidative stressors. Since 2012, she has been a Postdoctoral Scholar in an analytical research lab at Vanderbilt University, continuing immunological response research. Her current research utilizes the MAMP to study the role of anti-inflammatory and pro-inflammatory compounds that determine disease progression and intensity.

Sven E. Eklund received his PhD in Analytical Chemistry from the University of Tennessee in 1999 followed by postdoctoral research in the Department of Chemistry at Vanderbilt University where he performed some of the initial work on the MAMP. He is presently an Associate Professor of Chemistry at Louisiana Tech University where his research interests include fluorescence-based biosensors for multianalyte microphysiometery, electrokinetic nanoparticle treatment of porous materials, and electrodeposition of refractory metals from ionic liquids.

David E. Cliffel received a B.S. in Chemistry and a Bachelor of Electrical Engineering from the University of Dayton in 1992. He received his Ph.D. in chemistry in 1998 from the University of Texas at Austin under the direction of Professor Allen J. Bard and did postdoctoral work with Professor Royce W. Murray at the University of North Carolina as a postdoctoral associate working on the electrochemistry of monolayer protected clusters. His current research as an Associate Professor at Vanderbilt University concentrates on the electrochemical analysis of nanoparticles and of biological cells using scanning electrochemical microscopy and continues the development of the multianalyte microphysiometer for metabolic profiling and toxicology and for sensing and control of organs-on-chips.

John P. Wikswo received the B.A. degree from the University of Virginia in 1970 and M.S. and Ph.D. degrees, all in physics, from Stanford University in 1973 and 1975, respectively. He joined the Vanderbilt University faculty in 1977, where he is now the Gordon A. Cain University Professor, the A. B. Learned Professor of Living State Physics, and Professor of Biomedical Engineering, Molecular Physiology and Biophysics, and Physics, and the founding Director of the Vanderbilt Institute for Integrative Biosystems Research and Education. He uses novel instrumentation, quantitative measurements, and mathematical models to study and control cellular metabolism and signaling in organs on chips.

Highlights

- Development of a novel multipotentiostat system
- Capable of measuring simultaneous amperometric and potentiometric signals in up to six individual cells
- Low levels of crosstalk between instruments used in conjunction
- Software and modular design allows for flexibility for future experimental needs

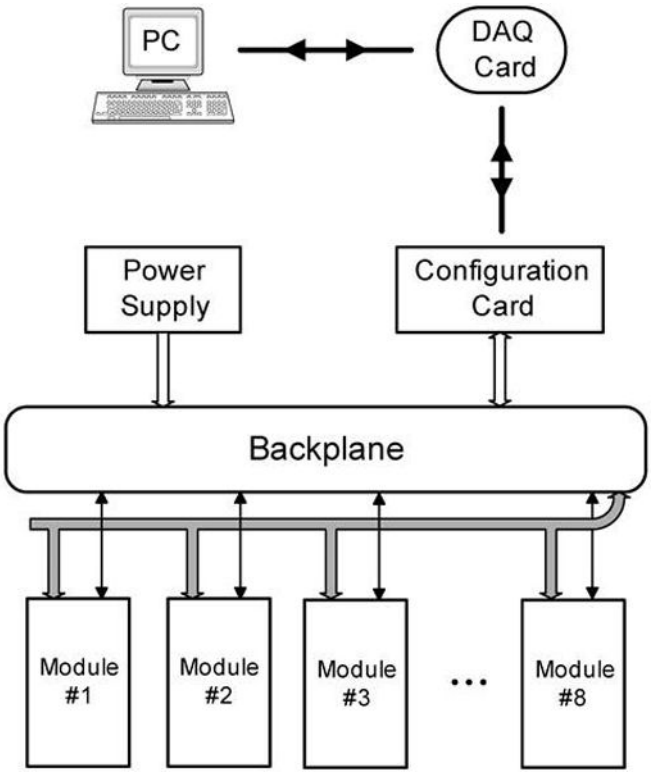

Figure 1.
Multichamber multipotentiostat system schematic.

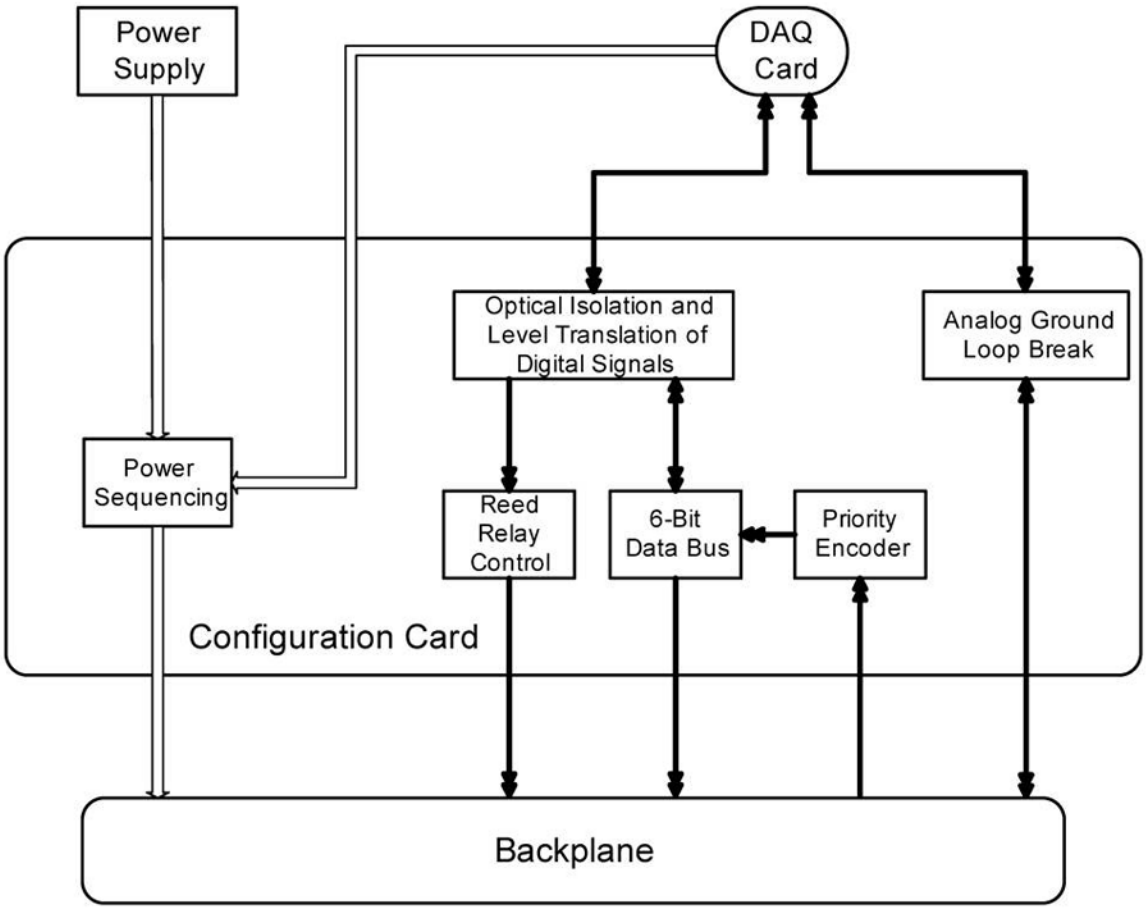

Figure 2.
Configuration card schematic.

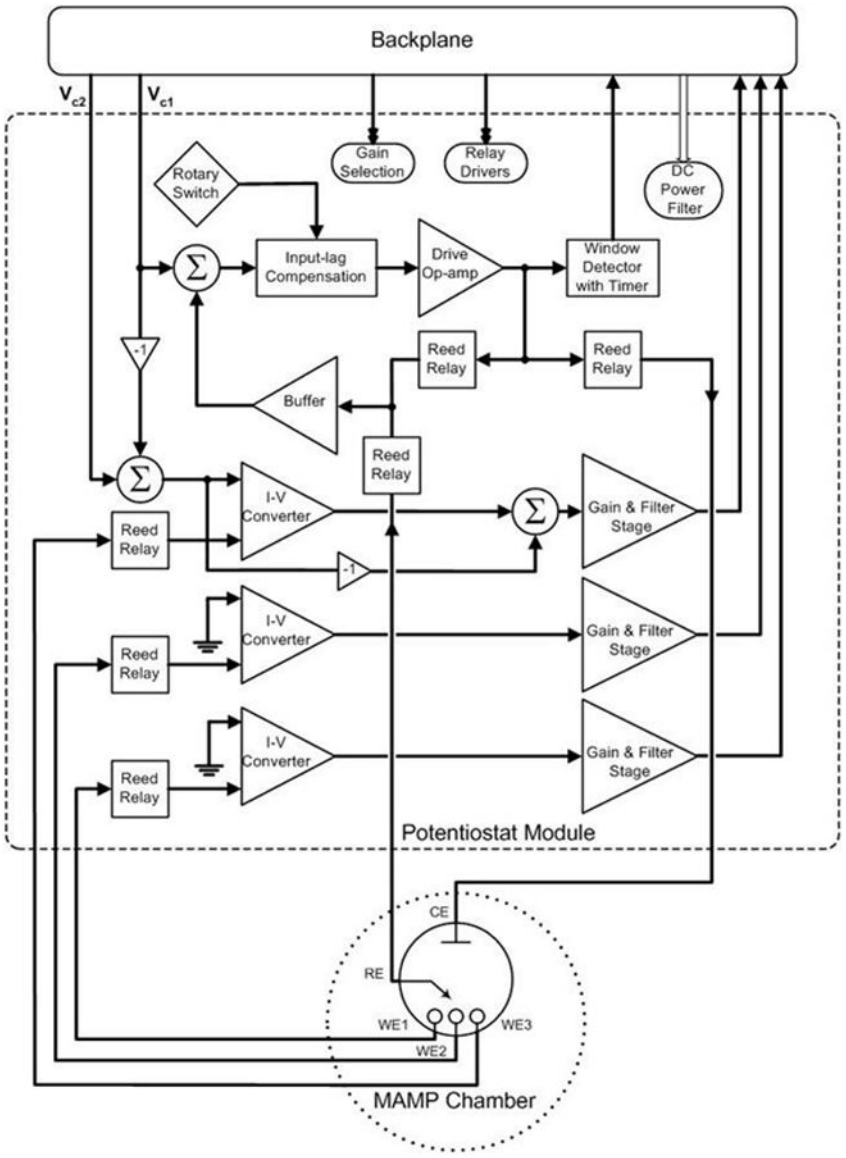

Figure 3.

Multipotentiostat module schematic. The MAMP chamber features three Wes (circles), one RE (arrow), and one CE (line).

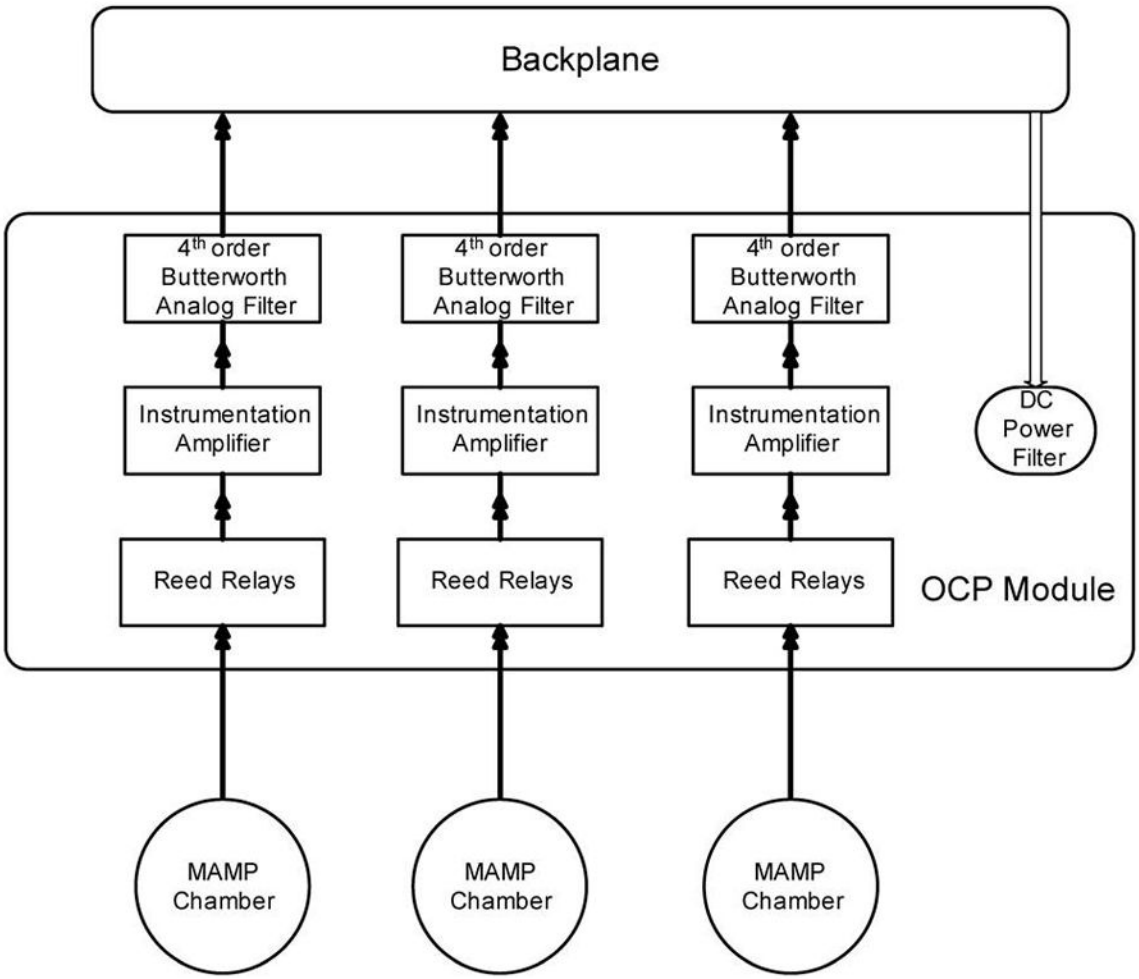

Figure 4.
OCP module schematic.

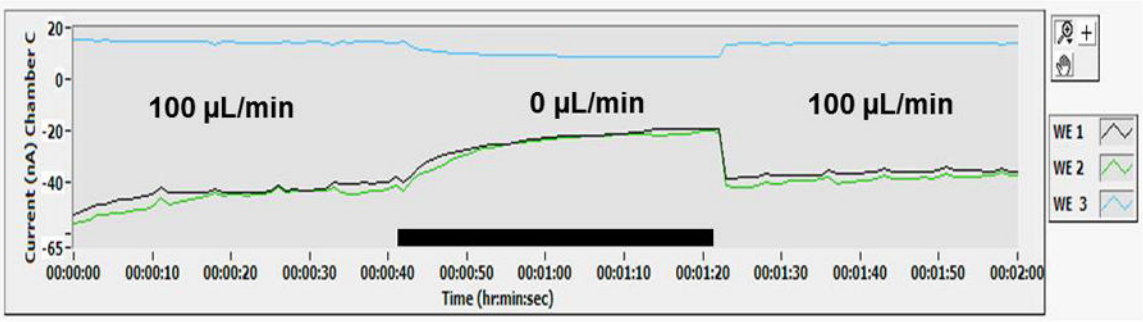

Figure 5.

LabVIEW™ multipotentiostat interface of a typical current response at a modified sensor head without cells in the chamber. Sensors were assembled in the chamber and perfused with media. At 00:00:40, flow is stopped for 40s (black bar). 100µL/min flow of media resumed at 00:01:20, reestablishing baseline current.

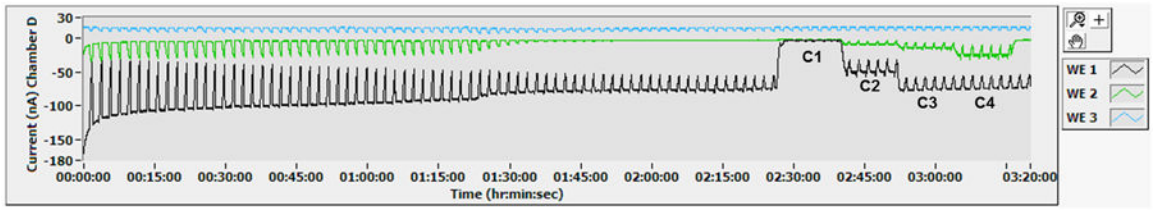

Figure 6.

Typical current response at modified sensor head during MAMP experiment. Enzymatically coated sensors were assembled in each chamber with 5×10^5 PC-12 cells and perfused with media. At 01:20:00, perfusion of media containing 108μM alamethicin initiated cell death and calibrations were performed (C1: 0mM glucose and lactate; C2: 1mM glucose, 0.05mM lactate; C3: 3mM glucose, 0.1mM lactate; C4: 5mM glucose, 0.2mM lactate).

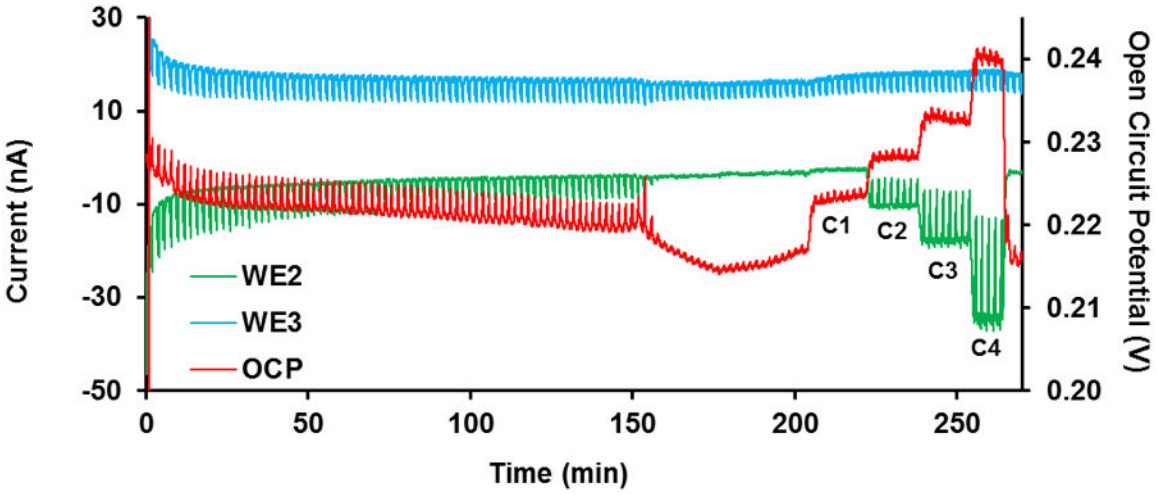

Figure 7.

Typical current and OCP response at a modified sensor head during MAMP experiment. Sensors with electrode coatings were assembled in a Cytosensor® chamber with neuronal cultures and perfused with media. At 150min, perfusion of media containing 75μM alamethicin initiated cell death and calibrations were performed (C1: 0mM lactate, pH 7.48; C2: 0.05mM lactate, pH 7.31; C3: 0.1mM lactate, pH 7.21; C4: 0.2mM lactate, pH 7.08).

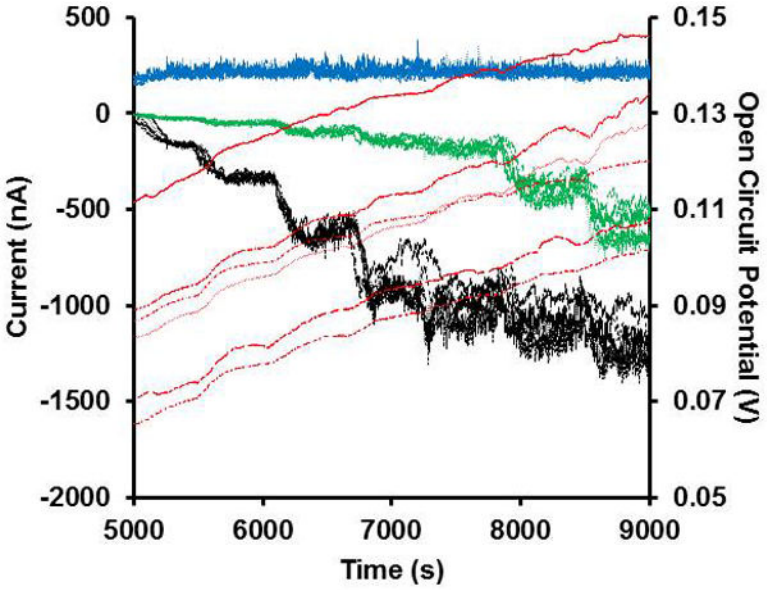

Figure 8.

Typical current and OCP response at an array of 4-analyte SPEs. Sensors with electrode coatings were calibrated together in PBS with additions of glucose, lactate, and acid in 10 steps up to 16mM glucose, 1mM lactate, and pH 7.4 to 7.0. Glucose is in black, lactate in green, oxygen in blue, pH in red.